Electronic Supplementary Information for

Two-dimensional Multiferroic RuClF/$AgBiP_2S_6$ van der Waals Heterostructure with Valley Splitting Properties and Controllable Magnetic Anisotropy

Ziyu Liu,[a] Baozeng Zhou[a] and Xiaocha Wang[a,*]

[a]*Tianjin Key Laboratory of Film Electronic & Communicate devices, School of Integrated Circuit Science and Engineering, Tianjin University of Technology, Tianjin 300384, China*

[*]Author to whom all correspondence should be addressed.

E-mail: wangxc@email.tjut.edu.cn

Table S1. The formation energies of RuClF and AgBiP2S6 monolayers and the chemical potentials of each element.

	μ_{Ru}	μ_{Cl}	μ_{F}	μ_{Ag}	μ_{Bi}	μ_{P}	μ_{S}	E_f
RuClF	-9.210	-1.842	-1.857	/	/	/	/	-1.058
$AgBiP_2S_6$	/	/	/	-32.212	-4.606	-5.083	-2.515	-0.571

Table S2. The total energy (eV) of RuClF/ $AgBiP_2S_6$ heterostructures with different magnetic configuration.

Polarization	AFM-1	AFM-2	AFM-3	FM
P↑	-94.570861	-94.570573	-94.570635	-94.601326
P↓	-94.527509	-94.527379	-94.527423	-94.557960

Table S3. Ferroelectric dipole moments, paraelectric dipole moments and polarization intensities of $AgBiP_2S_6$ and $RuClF/AgBiP_2S_6$ heterostructures.

	p_{zFE}	p_{zPE}	P_Z (10^{-10}C/m^2)
$AgBiP_2S_6$	-28.31796	-28.78903	0.17994
$RuClF/AgBiP_2S_6$-P↑	-67.47134	-39.35030	12.16129
$RuClF/AgBiP_2S_6$-P↓	-56.24972	-87.37059	-12.16122

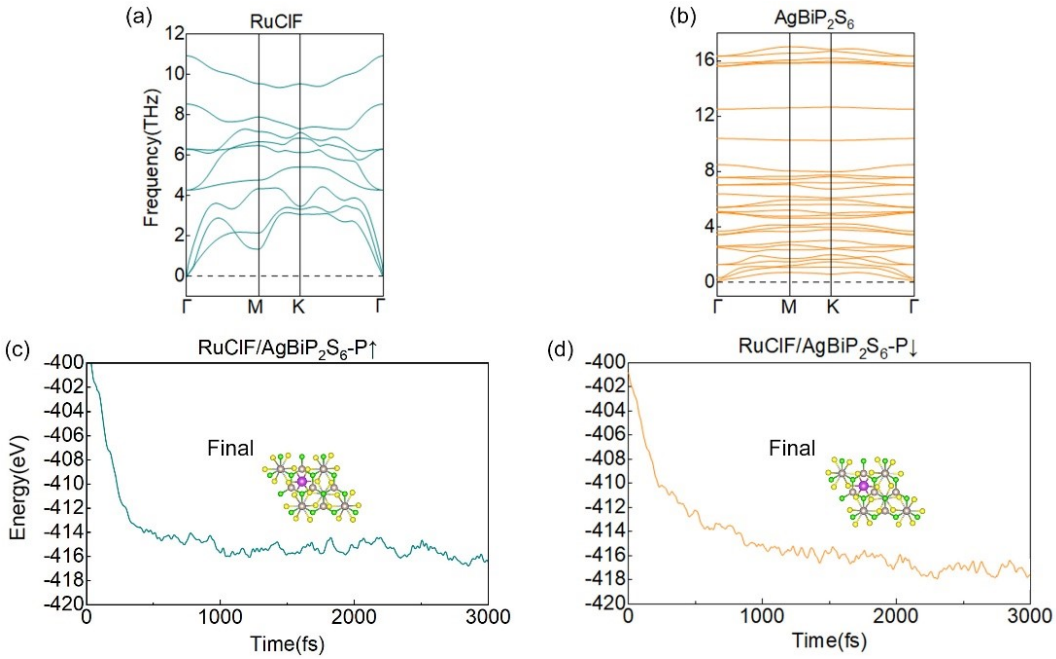

Fig. S1 Phonon spectrum of (a) RuClF and (b) $AgBiP_2S_6$ monolayers. (c)-(d) Simulation of potential energy fluctuations in RuClF/$AgBiP_2S_6$ heterostructures in the different polarizations after 3ps.

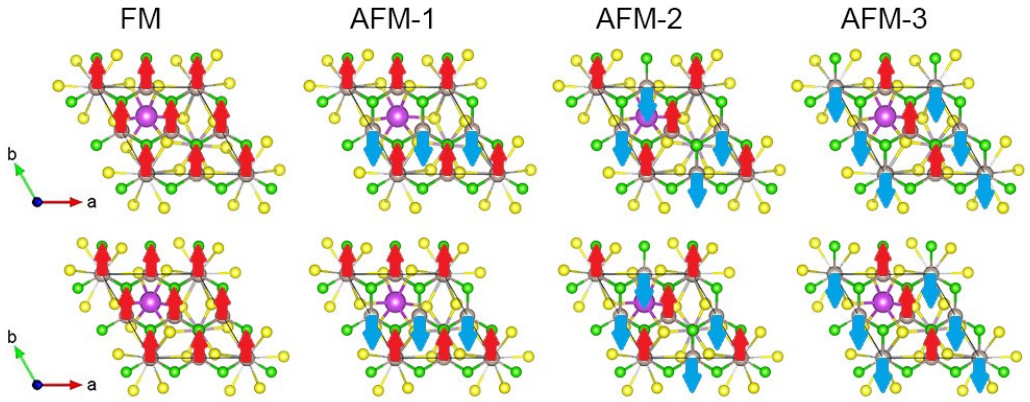

Fig. S2 The structures of two kinds of RuClF/$AgBiP_2S_6$ heterostructures in FM, AFM1, AFM2 and AFM3 states. Red and Blue arrows indicate different spin directions.

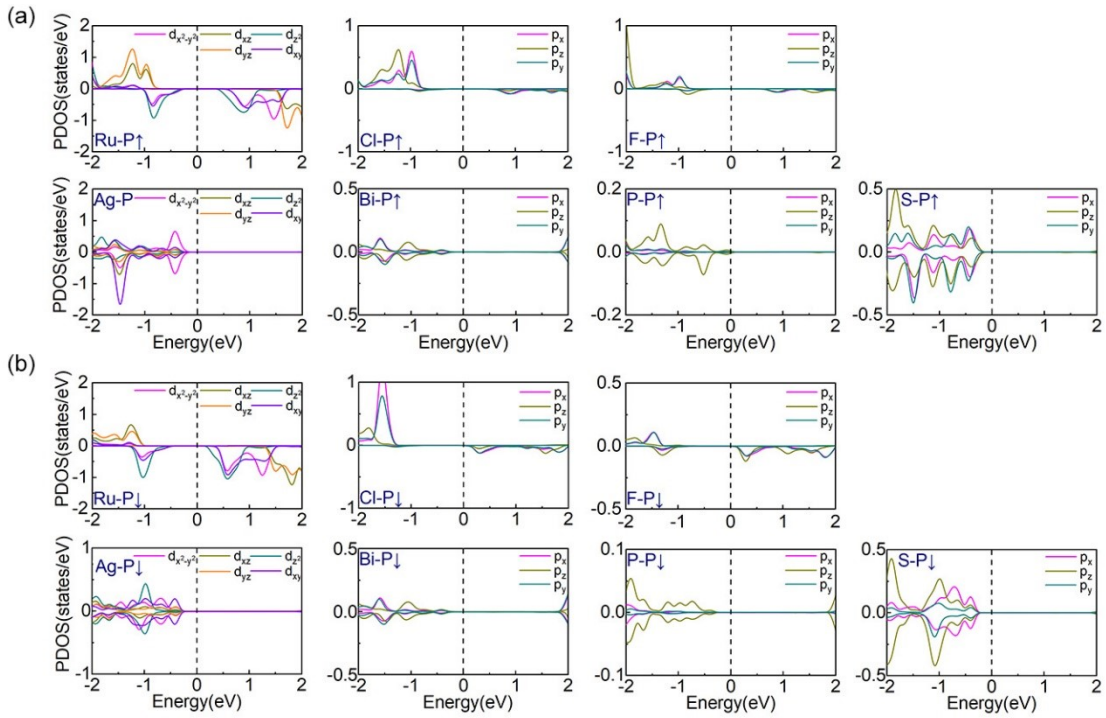

Fig. S3 (a)-(b) DOS of each element of RuClF/$AgBiP_2S_6$ heterostructures in different polarizations. The Fermi level is set as 0eV.

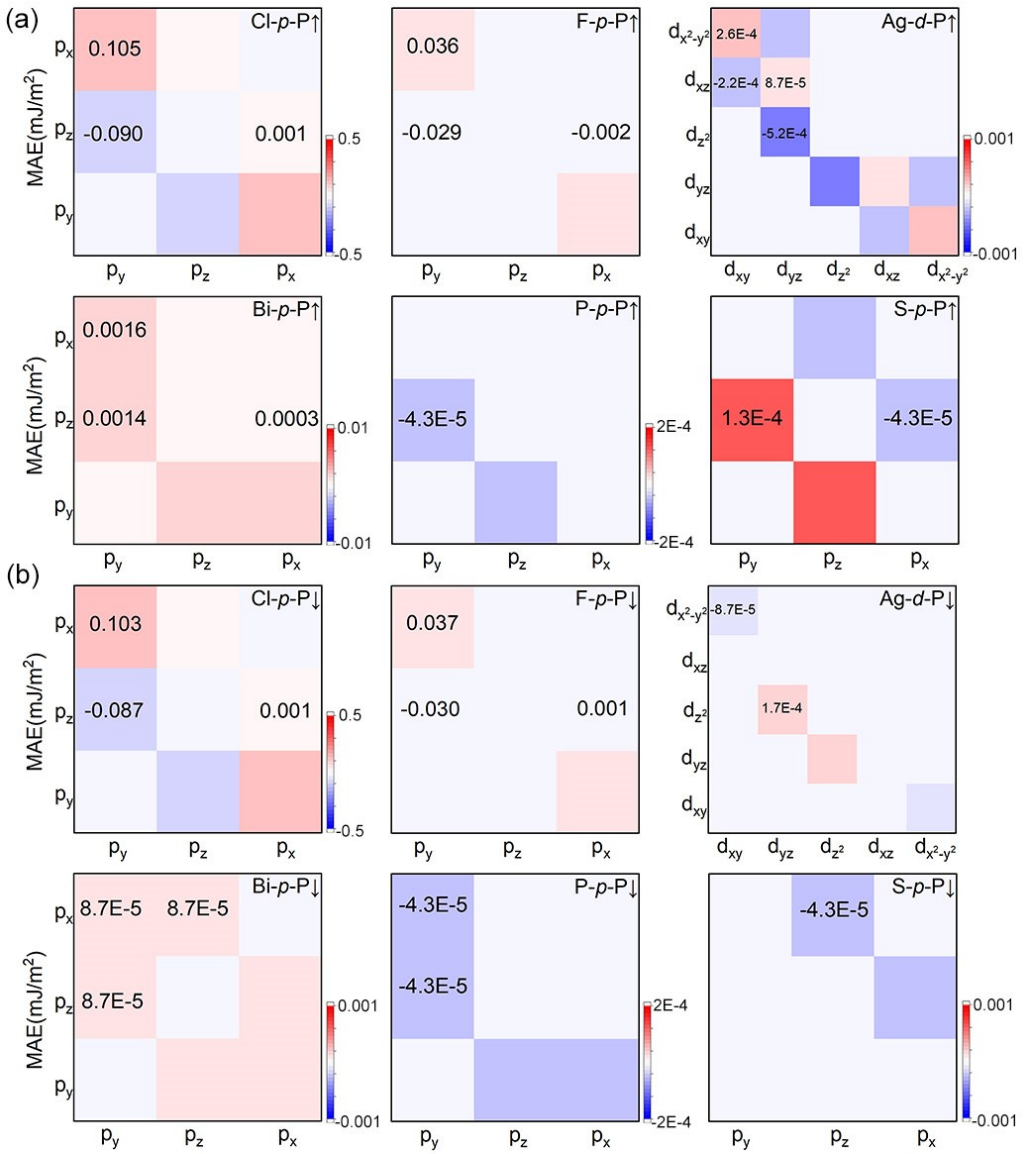

Fig. S4 (a)-(b) Each element (except Ru)'s orbital resolved MAE of RuClF/$AgBiP_2S_6$ heterostructures in different polarizations.

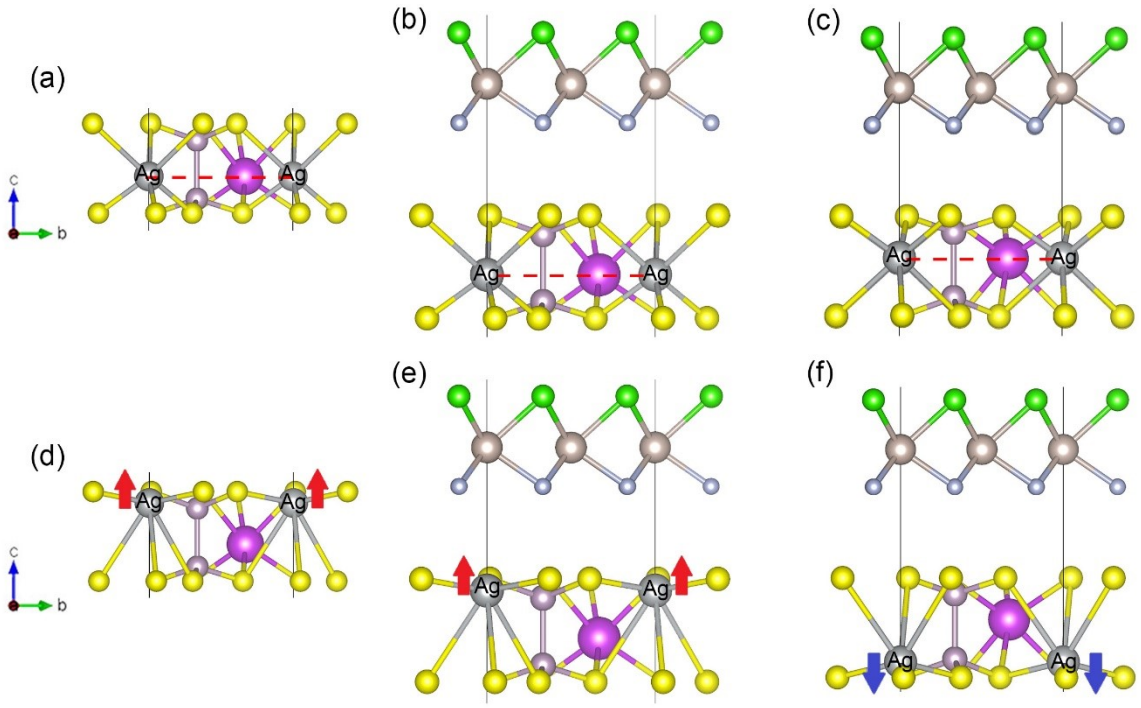

Fig. S5 Paraelectric phase structures and ferroelectric phase structures of $AgBiP_2S_6$ and RuClF/$AgBiP_2S_6$ heterostructures.

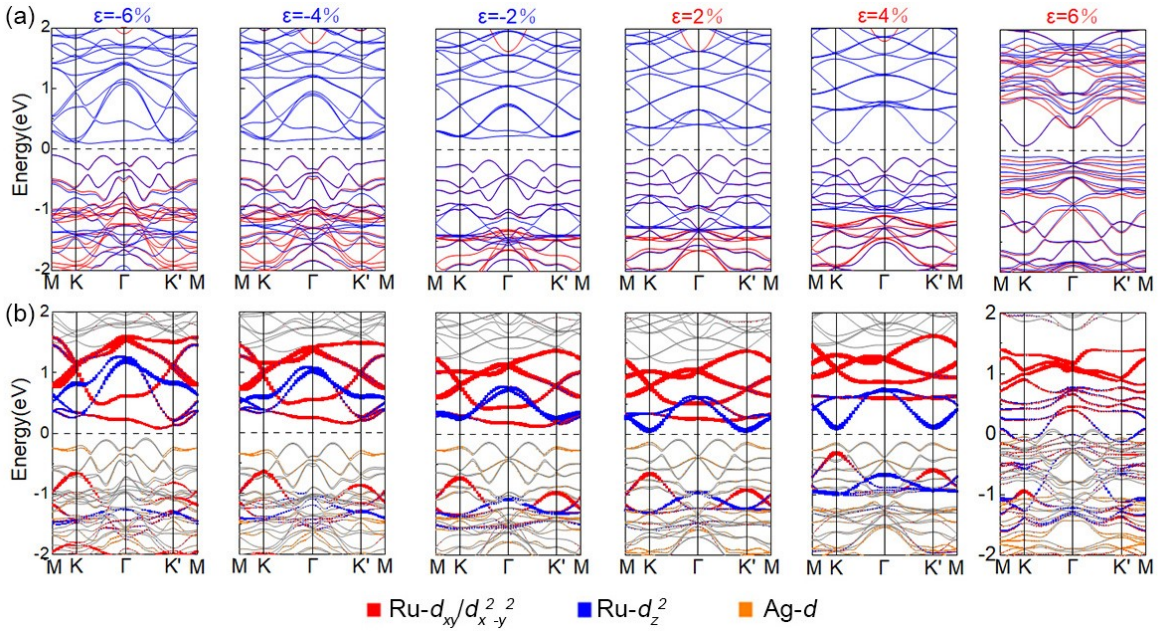

Fig. S6 Band structures (a)without and (b)with SOC of RuClF/$AgBiP_2S_6$-P↓ heterostructure at different biaxial strains.